Heliyon 9 (2023) e15451

Contents lists available at ScienceDirect

Heliyon

journal homepage: www.cell.com/heliyon

Research article

miR-21-5p prevents doxorubicin-induced cardiomyopathy by downregulating BTG2

Qingwei Wang [a,1], Fei Jiang [b,1], Chenglin Zhao [c,1], Jiaxin Song [c], Meiyu Hu [c], Yicheng Lv [c], Yi Duan [c], Wenqian Fang [c], Rongjing Ding [d,**], Yan Qiu [c,*]

[a] Department of Cardiology, People's Hospital, Peking University, Beijing, 100044, China
[b] Heart Medicine Research Center, Fujian Medical University Union Hospital, Fuzhou, 350001, Fujian, China
[c] Shanghai Engineering Research Center of Organ Repair, School of Medicine, Shanghai University, Shanghai, 200444, China
[d] Cardiac Rehabilitation Center, Department of Rehabilitation Medicine, Peking Union Medical College Hospital, Beijing, 100730, China

ARTICLE INFO

Keywords:
miR-21-5p
DOX-induced cardiomyopathy
Cardiomyocyte apoptosis
BTG2

ABSTRACT

Cardiomyocyte apoptosis has been characterized as one of the major mechanisms underlying doxorubicin (DOX)-induced cardiomyopathy. MicroRNA-21-5p (miR-21-5p) was reported to mitigate ischemia-induced cardiomyocyte apoptosis and cardiac injury. However, to our knowledge, the functional role of miR-21-5p in DOX-induced cardiomyopathy is unclear. In this study, we explored the role of miR-21-5p in DOX-induced cardiac injury. The expression level of miR-21-5p was detected by quantitative real-time polymerase chain reaction (qRT-PCR). Dual luciferase reporter assay was used to verify the potential target gene of miR-21-5p. The apoptosis rate of NRCMs was detected by TUNEL staining assay. Western blot analysis was used to detect the protein expression levels of Bax, Bcl-2, Caspase3, cleaved-Caspase3 and BTG2. For animal studies, mice were injected with AAV9-miR-21-5p or AAV9-Empty viruses, and treated with DOX at a dose of 5 mg/kg per week through intraperitoneally administration. After 4 weeks of DOX treatment, mice were subjected to echocardiography to measure the left ventricular ejection fraction (EF) and fractional shortening (FS). Results showed that miR-21-5p was upregulated in both DOX-treated primary cardiomyocytes and mouse heart tissues. Interestingly, enhanced miR-21-5p expression inhibited DOX-induced cardiomyocyte apoptosis and oxidative stress, while decreased miR-21-5p expression promoted cardiomyocyte apoptosis and oxidative stress. Furthermore, cardiac overexpression of miR-21-5p protected against DOX-induced cardiac injury. The mechanistic study indicated that BTG2 was a target gene of miR-21-5p. The anti-apoptotic effect of miR-21-5p could be inhibited by BTG2 overexpression. Conversely, inhibition of BTG2 rescued the pro-apoptotic effect of miR-21-5p inhibitor. Taken together, our study showed that miR-21-5p could prevent DOX-induced cardiomyopathy by downregulating BTG2.

Abbreviations: AAV9, Adeno-associated virus serotype 9; BTG2, B cell translocation gene 2; DOX, Doxorubicin; Drp1, Dynamic-related protein-1; EF, Ejection fraction; FS, Fractional shortening; HL, Tibial length; H/R, Hypoxia-reperfusion; HW, Heart weight; I/R, Ischemia-reperfusion; miRs, MicroRNAs; MOI, Multiplicities of infection; NRCMs, Neonatal rat cardiomyocytes; PGC-1α, Peroxisome proliferator-activated receptor-gamma coactivator-1α; qRT-PCR, Quantitative real-time polymerase chain reaction; snRNA, Small nuclear RNA; TAF9b, TATA-binding protein associated factor 9b; TUNEL, Terminal deoxyribonucleotidyl transferase (TdT)-mediated dUTP nick end labeling; 3'UTR, 3'Untranslated region.

* Corresponding author.
** Corresponding author.
E-mail addresses: drj2003@vip.163.com (R. Ding), qiuyan@shu.edu.cn (Y. Qiu).
[1] These authors contributed equally to this work.

https://doi.org/10.1016/j.heliyon.2023.e15451
Received 9 February 2023; Received in revised form 27 March 2023; Accepted 10 April 2023
Available online 19 April 2023

1. Introduction

Doxorubicin (DOX) is a class of anthracycline antibiotics widely used in the treatment of various types of cancer, such as leukemia, lymphoma, solid malignant tumors, etc. However, the administration of anthracyclines always causes dose-dependent and cumulative cardiotoxicity, which eventually leads to transient cardiac dysfunction and even congestive heart failure, severely restrict their clinic use [1–3]. With the growing number of cancer survivors, there is an increasing need to develop preventive strategies and effective treatments against DOX-induced cardiac injury. Although extensive basic and clinical investigations on DOX-induced cardiotoxicity have continued for decades, the underlying mechanisms of DOX-induced cardiotoxicity are still incompletely understood.

Numerous studies have elucidated the potential molecular mechanisms that are responsible for the development of DOX-induced cardiotoxicity. They include molecular pathways related to mitochondrial dysfunction, oxidative stress, calcium dysfunction, iron-free radical production, apoptosis, immune system, etc [4–6]. Of note, the production of free radicals has been recognized as the main cause of cardiac injury induced by DOX [7–9]. However, interventions aimed to reduce oxidative stress did not succeed in reducing the incidence of DOX-induced cardiomyopathy [10]. Therefore, it is urgent to further understand the pathogenesis of DOX-induced cardiomyopathy and find out new therapeutic targets.

A large body of evidence supports the notion that the death of terminally differentiated cardiomyocytes is one of the key pathogenic factors in the development of cardiac injury [11]. Of all the types of regulated cell death, cardiomyocyte apoptosis has been considered to be the main characterization of DOX-induced cardiomyopathy [12]. A low concentration of DOX can induce the apoptosis of cardiomyocytes and ultimately leads to heart failure [3]. Studies have shown that DOX-induced oxidative stress can directly trigger a large number of cardiomyocyte apoptosis through external and internal apoptotic pathways, leading to severe cardiac dysfunction [10, 13]. Importantly, inhibition of myocardial cell apoptosis can significantly prevent DOX-induced cardiac dysfunction [14,15]. Hence, further in-depth exploration of the molecular mechanism that regulates cardiomyocyte apoptosis is of great significance for the discovery of new therapeutic targets for DOX-induced cardiomyopathy.

MicroRNAs (miRNAs, miRs) are small non-coding RNA molecules with a length of about 19–25 nucleotides, which can regulate gene expression at the post-transcriptional level by inhibiting the translation or promoting the degradation of target mRNA [16]. Accumulating evidence shows that miRNAs play key roles in the development of cardiovascular diseases, and miRNAs are proposed as potential drug targets for the treatment of human cardiovascular disease [17–23]. Particularly, miRNAs mediate multiple pathways that are potential targets for cardioprotection against DOX, including p53 signaling, pro-survival signaling, mitochondrial function, etc [24]. For example, inhibition of miR-140-5p alleviates DOX-induced cardiac myocardial oxidative damage [25]. Downregulation of miR-23a attenuates DOX-induced cardiomyocyte damage via targeting the peroxisome proliferator-activated receptor-gamma coactivator-1α (PGC-1α)/dynamic-related protein-1 (Drp1) pathway [26]. Additionally, miR-146a could decrease apoptosis and improve autophagy in cardiomyocytes via targeting TATA-binding protein associated factor 9b (TAF9b)/p53 pathway, thereby inhibiting DOX-induced cardiotoxicity [27].

Here we aimed to explore whether miR-21-5p plays a cardioprotective role in DOX-induced cardiotoxicity. miR-21-5p is expressed in basically all kinds of human cells and is reported to have important regulatory roles in health and disease, and it is also one of the most commonly studied miRNAs in cardiovascular disease and neoplasias [28,29]. Evidence showed that miR-21-5p had a protective effect on ischemia-hypoxia-induced cardiomyocyte apoptosis [30,31]. Moreover, it is reported that miR-21-5p promoted angiogenesis and cardiomyocyte survival through phosphatase and tensin homolog/Akt pathways, thereby promoting heart repair mediated by exosomes [31]. In addition, a previous study reported that DOX treatment significantly upregulated miR-21-5p levels in both mouse heart tissues and H9C2 cells [32]. Increased miR-21-5p expression prevented DOX-induced apoptosis in *in-vitro* cultured cardiomyocytes while decreased miR-21-5p expression promoted DOX-induced apoptosis. And B cell translocation gene 2 (BTG2) was reported to be a target gene of miR-21-5p in cardiomyocytes [32]. However, the *in vivo* investigation of the functional roles of miR-21-5p is lacking. As a result, in this study, we investigated the functional role of miR-21-5p in the murine model of DOX-induced cardiotoxicity and DOX-induced apoptosis model of cardiomyocytes. We further investigated target gene and molecular mechanisms underlying the myocardial protective effect of miR-21-5p.

2. Materials and methods

2.1. Animals and treatment

Thirty-three male C57BL/6J wild-type mice, aged eight-week-old (weight 24–25 g), were purchased from Shanghai Laboratory Animal Center (SLAC, Shanghai, China) and housed in autoclaved ventilated cages with sterile food and water ad libitum. All animal experiments were conducted under the established guidelines on the use and care of laboratory animals for biomedical research published by the National Institutes of Health (No. 85-23, revised 1996) and approved by the ethical committees of Shanghai University (approval number ECSHU 2021-074).

To mimic DOX-induced cardiomyopathy, mice were injected intraperitoneally with DOX (Sigma, USA) at a dose of 5 mg/kg once a week for four weeks. DOX powder was dissolved in physiological saline with the stock concentration at 0.5 mg/mL, and then stored to avoid light at 4 °C. The control mice were administrated with an equal volume of saline. To study the preventive effect of miR-21-5p *in vivo*, Adeno-associated virus serotype 9 (AAV9) expressing miR-21-5p (AAV9-miR-21-5p) was injected through the tail vein at a dose of 1×10^{12} vg per mouse. AAV9-miR-21-5p and control viruses (AAV9-Empty) were purchased from Hanbio Biotechnology (Shanghai, China). For cardiac expression of miR-21-5p, mouse miR-21-5p was inserted between *Bam*HI and *Eco*RI restriction enzyme sites of the

pHBAAV-CMV-MCS-3 flag-T2A-ZsGreen vector (Hanbio Biotechnology). And construct was verified by sequencing before using. AAV9-miR-21-5p viruses were generated using packaging plasmids AAV2/9 (Hanbio Biotechnology) and Helper (Hanbio Biotechnology) together with AAV-CMV-miR-21-5p construct in HEK293T cells. AAV viral particles were collected from the HEK293T cell at 72 h post-transfection. Viral pellets were then purified using the AAV purification maxi kit (Biomiga, V1469-01) and tittered by qRT-PCR. DOX-induced mouse cardiac injury model was established one week after AAV9-miR-21-5p virus delivery. Five weeks later, mice were sacrificed by cervical dislocation for further analysis.

2.2. Echocardiography

Echocardiography was performed on the mice using a Vevo 2100 (VisualSonics, Ontario, Canada) with a 30 MHz central frequency scan-head. The mice were anesthetized with 3% isoflurane, and 1%–1.5% of isoflurane was used to maintain the anesthesia. Left ventricular ejection fraction (EF) and fractional shortening (FS) were measured from M-mode images taken from the parasternal short-axis view at the papillary muscle level.

2.3. Cardiomyocyte isolation, culture, and treatment

Cardiomyocytes were isolated from neonatal rats as described previously [33]. Isolated primary neonatal rat cardiomyocytes (NRCMs) were purified by Percoll gradient centrifugation. Before treatment, NRCMs were cultured in Dulbecco's modified Eagle's medium (DMEM, Corning, 22,517,004) supplemented with 10% horse serum (Gibco, 16050-122) and 5% fetal bovine serum (Biological industries, 04-001-1ACS) at 37 °C under 5% CO_2. miR-21-5p mimic or miR-21-5p inhibitor and their respective negative controls were purchased from RiboBio (Guangzhou, China). The sequences for miR mimic and inhibitor were listed in the Supplemental Table S2. miR-21-5p mimic (50 nM), miR-21-5p inhibitor (100 nM), and their respective negative controls were transfected into NRCMs with Lipofectamine™ 2000 (Invitrogen, MA, USA) according to the manufacturer's instructions, and incubated at 37 °C under 5% CO_2 for 6–8 h. Subsequently, the transfection medium was changed with serum-free medium. After 24 h of the transfection, NRCMs were treated with DMEM containing DOX (0.3 μM) under dark conditions for 24 h.

The DNA fragment encoding rat BTG2 was amplified from rat heart genomic complementary DNA (cDNA) and cloned into the FUGW cloning vector. The resultant construct was named pFUGW-BTG2. The shRNA sequence for BTG2 is 5′-CCGGGGACGCACTGACCGATCATTACTCGAGTAATGATCGGTCAGTGCGTCCTTTTTG-3′ and was cloned into the pLKO.1-TRC cloning vector. The resultant construct was named pLKO.1-shBTG2. The sh-BTG2 lentiviruses were packaged using the second generation packaging system plasmids psPAX2 (AddGene, 12260) and pMD2.G (AddGene, 12259) together with pLKO.1-shBTG2 construct. The 293T cells were purchased from Cell bank (Type Culture Collection Committee, Chinese Academy of Sciences, Shanghai) and cultured in DMEM containing 10% FBS in a humidified incubator with 5% CO_2 at 37 °C. To produce sh-BTG2 lentiviruses, HEK293T cells in each 10 cm dish were transfected with 1.25 μg pMD2.G, 3.75 μg psPAX2 and 5 μg pLKO.1-shBTG2 using polyethylenimine (kingmorn, KE1098). Medium was changed 12 h after transfection. Lentiviral supernatants were collected at 48 and 72 h post-transfection and stored at 4 °C for immediate use or −80 °C for longer use. The BTG2 overexpressing lentiviruses were packaged using packaging plasmids psPAX2 and pMD2.G together with the pFUGW-BTG2 construct. To produce BTG2 overexpressing lentiviruses, HEK293T cells in each 10 cm dish were transfected with 1.25 μg pMD2.G, 3.75 μg psPAX2 and 5 μg pFUGW-BTG2. All other steps are identical to the procedure of sh-BTG2 lentiviruses production. NRCMs were treated with lentiviruses for 72 h with 10 MOI (Multiplicities of infection) and then used for subsequent experiments.

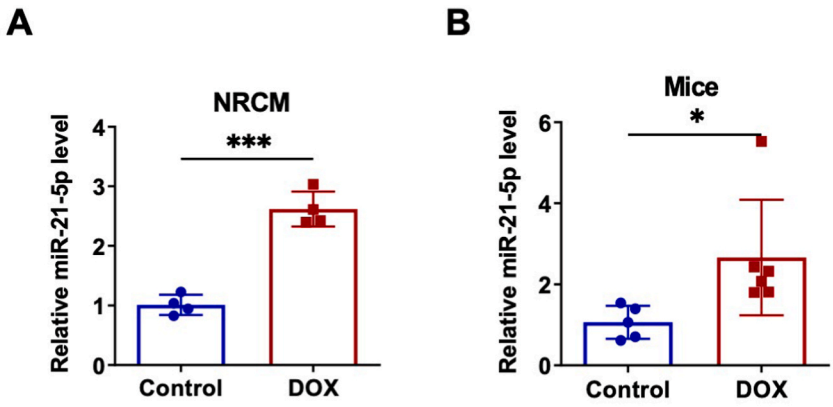

Fig. 1. miR-21-5p was upregulated in DOX-treated primary neonatal rat cardiomyocytes and mouse heart tissues. **A** qRT-PCR analysis of miR-21-5p level in primary neonatal rat cardiomyocytes (NRCMs) treated with or without Doxorubicin (DOX). n = 4. **B** qRT-PCR analysis of miR-21-5p level in control and DOX-treated mouse heart tissues. n = 5:6. Bars show mean ± SD. Data between two groups were compared by unpaired two-tailed student's *t*-test. *, $p < 0.05$, ***, $p < 0.001$.

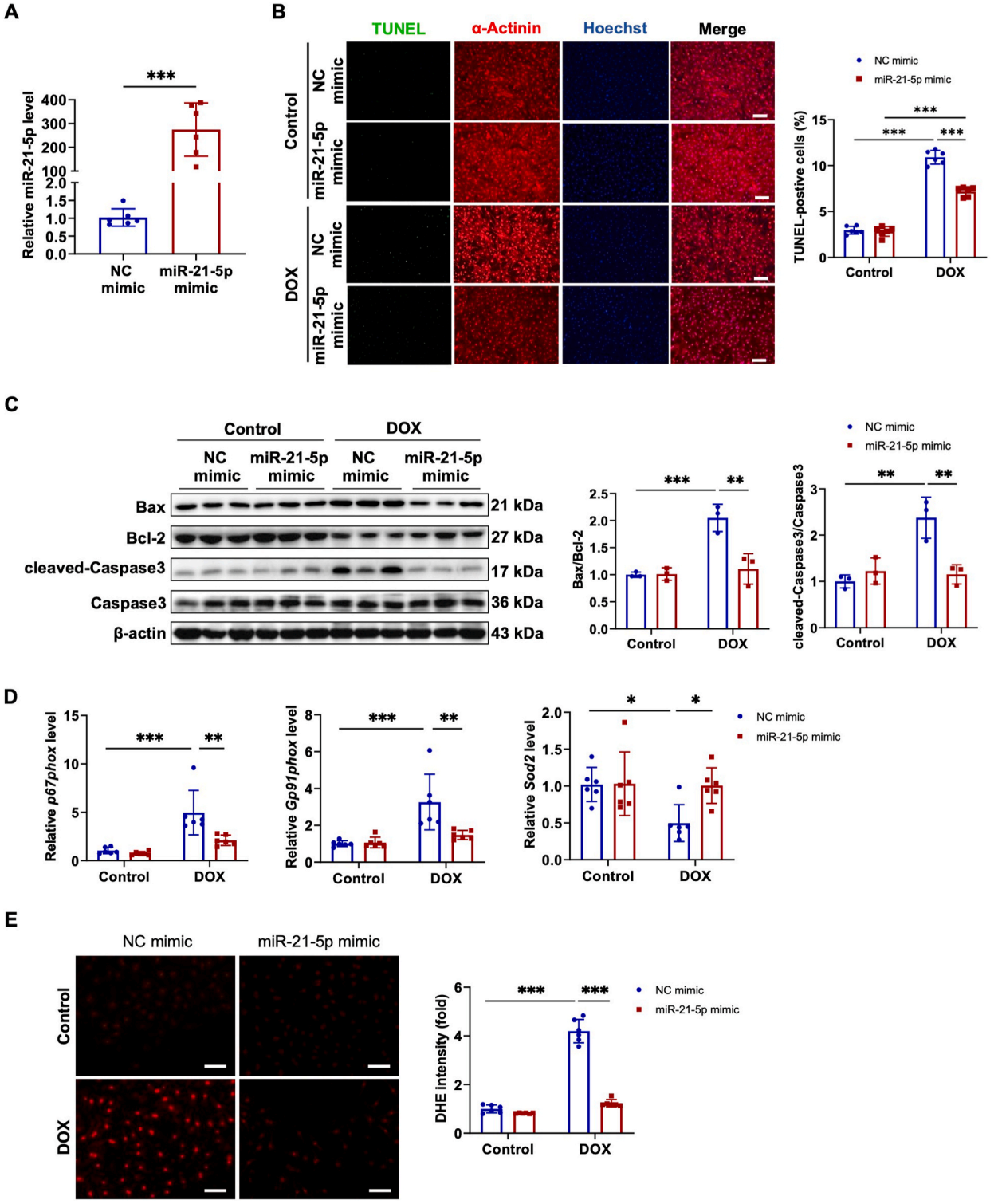

(caption on next page)

Fig. 2. Overexpression of miR-21-5p prevented DOX-induced cardiomyocyte apoptosis and oxidative stress. **A** qRT-PCR analysis of miR-21-5p expression in primary neonatal rat cardiomyocytes (NRCMs) transfected with NC mimic or miR-21-5p mimic. n = 6. **B** TUNEL staining for α-actinin-labeled NRCMs transfected with NC mimic or miR-21-5p mimic, and the statistical results. n = 6. **C** Western blot analysis of Bax, Bcl-2, cleaved-Caspase3, and Caspase3 levels in Doxorubicin (DOX)-treated NRCMs transfected with NC mimic or miR-21-5p mimic. n = 3. **D** qRT-PCR analysis of *p67phox*, *Gp91phox* and *Sod2* expression in NRCMs transfected with NC mimic or miR-21-5p mimic. n = 6. **E** Representative DHE staining images and statistical results. n = 6. Scale bar, 100 μm. Bars show mean ± SD. Data were compared by two-way ANOVA followed by Tukey's *post hoc* test. *, $p < 0.05$, **, $p < 0.01$, ***, $p < 0.001$. NC, negative control.

2.4. TUNEL staining assay

For terminal deoxyribonucleotidyl transferase (TdT)-mediated dUTP nick end labeling (TUNEL) staining analysis in heart tissues, frozen mouse heart sections were fixed with 4% paraformaldehyde for 15 min at room temperature, and next incubated in 20 μg/mL protease K at room temperature for 10 min. After washing with phosphate-buffered saline (PBS), heart tissue sections were incubated with the DeadEnd™ Fluorometric TUNEL system (Promega, Madison, WI, USA) for 1 h at 37 °C. After washing with PBS, nuclei were counterstained with 5 μg/mL Hoechst33342 (Beyotime Biotechnology, Shanghai, China) for 20 min at room temperature. Images were taken using a confocal microscope (Carl, Zeiss) under a magnification of 400 × , and at least 20 fields of view were observed by microscopy. Image J software was used for analysis.

For TUNEL staining analysis in NRCMs, TUNEL FITC Apoptosis Detection Kit (Vazyme, Nanjing, China) was used to fluorescently label the nuclei of apoptotic cells in accordance with the kit manufacturer's instructions. Subsequently, nuclei were counterstained with 5 μg/mL Hoechst33342 for 20 min at room temperature. Images were taken using a fluorescence microscope (Leica, Germany) under a magnification of 200 × , and at least 20 fields of view were observed by microscopy. Image J software was used for analysis.

2.5. RNA isolation and quantitative real-time polymerase chain reaction

Total RNA was extracted from cells or heart tissues using Trizol reagent (TaKaRa, Japan), and transcribed with the RevertAid first strand cDNA synthesis kit (ThermoScientific™, MA, USA) according to the manufacturer's protocol. The mRNA levels of *p67phox*, *Gp91phox*, *Sod2* were quantified using SYBR Green PCR Master Mix (Bio-Rad, USA) on a Real-Time PCR Detection System (Roche, Switzerland). The expression of miR-21-5p was detected using the Bulge-Loop™ miRNA qPCR Primer Set (RiboBio, Guangzhou, China). Reactions were performed at 95 °C for 5 min followed by 40 cycles at 95 °C for 5 s, and at 60 °C for 30 s, and at 72 °C for 30 s. Relative mRNA and miR-21-5p expression was normalized to the expression of 18s and U6 small nuclear RNA (snRNA) in cells and tissues using the $2^{-\Delta\Delta CT}$ method [34]. ΔCT = CT (target gene) – CT (18s/U6), ΔΔCT = ΔCT (experimental group) - ΔCT (control group). Primer sequences used in the present study are listed in Supplemental Table 1.

2.6. Western blot analysis

Total proteins were extracted from mouse heart tissues or NRCMs with radio immunoprecipitation assay (RIPA, KeyGen BioTECH, China) lysis buffer. The protein concentration was quantified by TaKaRa BCA Protein Assay Kit (TaKaRa, Japan). Equal amounts of protein (20–30 μg) were subjected to 12% sodium dodecyl sulfate-polyacrylamide gel electrophoresis (SDS-PAGE), and then transferred to a polyvinylidene fluoride membrane, and blocked with 5% BSA (KeyGen BioTECH, China) in Tris-buffered saline Tween (TBST, 0.1% Tween 20) for 2 h at room temperature. The membrane was then incubated with *anti*-cleaved-Caspase3 and *anti*-Caspase3 (1:1000, Abclonal, Wuhan, China, A11040), *anti*-Bax (1:1000, Abclonal, Wuhan, China, A12009), *anti*-Bcl-2 (1:1000, Abclonal, Wuhan, China, A19693), *anti*-BTG2 (1:1000, Abcam, Shanghai, China, ab197362), *anti*-GAPDH (1:1000, Bioworld, Nanjing, China, AP0063) and *anti*-β-actin (1:10000, Abclonal, Wuhan, China, AC004) at 4 °C overnight. Then, the *anti*-rabbit (1:10000, Jackson, USA, 111-035-003) or *anti*-mouse (1:10000, Bioworld, Nanjing, China, BS12478) second antibody was added and the membrane was incubated with the second antibody for 2 h at room temperature. The membrane was visualized in High-sig ECL Western Blotting Substrate (Tanon, Shanghai, China). Image J software was used for gray scale analysis.

2.7. Oxidative stress detection

ROS production was evaluated by DHE staining. For DHE staining analysis in heart tissues, frozen heart sections were washed with PBS and then stained with 30 μM DHE dye (KeyGen BioTECH, China) at room temperature for 30 min in a dark chamber. After washing with PBS, section were sealed with 50% glycerol avoid light and observed with a confocal microscope (Carl, Zeiss) under a magnification of 400 × . Image J software was used for analysis.

For DHE staining analysis in NRCMs, DHE dye (30 μM) (KeyGen BioTECH, China) was added to cardiomyocytes 30 min before termination of the experiment. Subsequently, cells were washed with fresh medium and incubated with PBS. Fluorescent images were observed with a fluorescence microscope (Leica, Germany) under a magnification of 200 × , and at least 20 fields of view were observed by microscopy. Image J software was used for analysis.

2.8. Dual-luciferase reporter assay

To study the direct interaction between miR-21-5p and the 3′UTR of BTG2, we constructed the luciferase reporter vector pGL3-

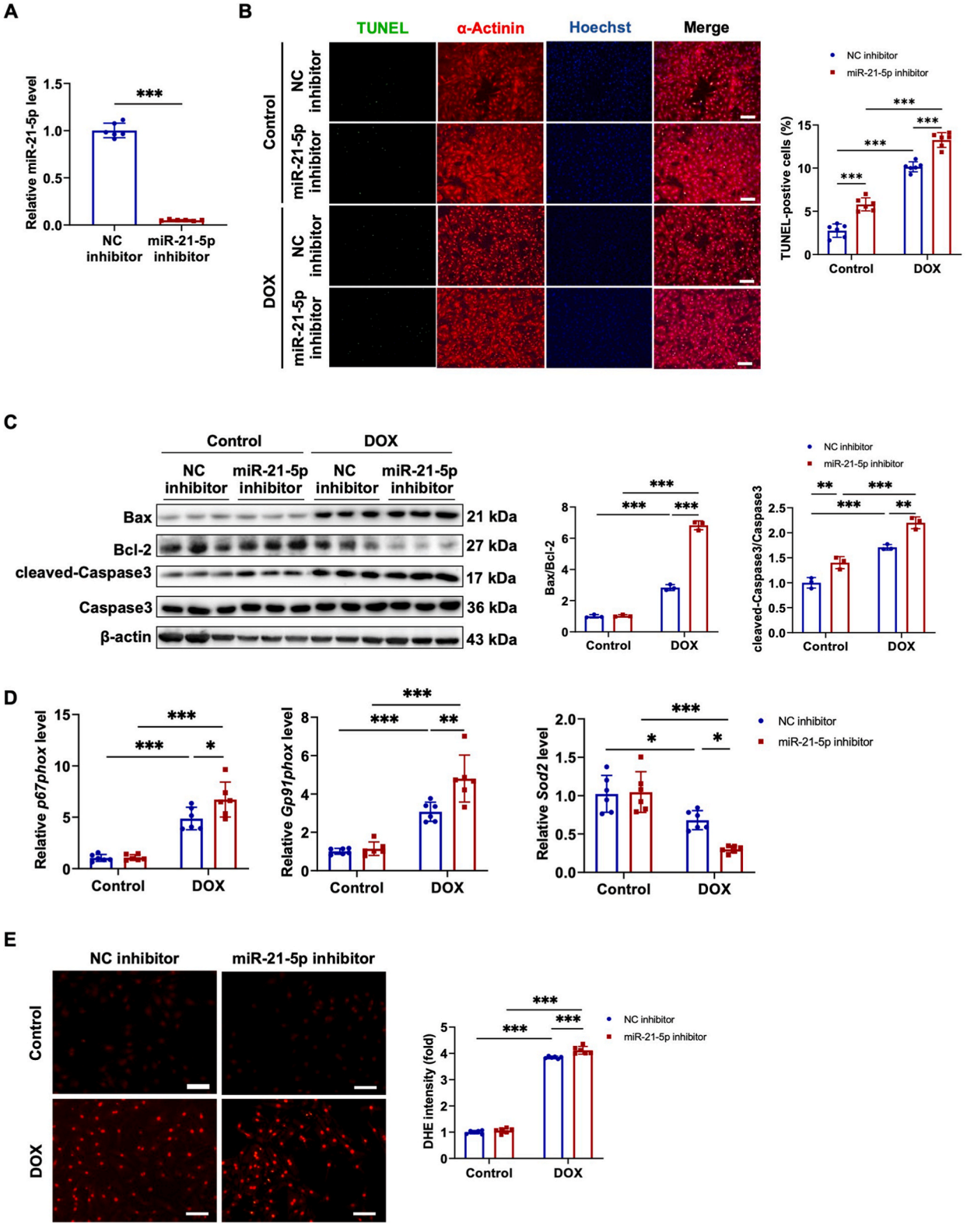

(caption on next page)

Fig. 3. miR-21-5p inhibition increased cardiomyocyte apoptosis and oxidative stress. **A** qRT-PCR analysis of miR-21-5p expression in primary neonatal rat cardiomyocytes (NRCMs) transfected with NC inhibitor or miR-21-5p inhibitor. n = 6. **B** TUNEL staining for α-actinin-labeled NRCMs transfected with NC inhibitor or miR-21-5p inhibitor. n = 6. **C** Western blot analysis of Bax, Bcl-2, Caspase3, and cleaved-Caspase3 levels in Doxorubicin (DOX)-treated NRCMs transfected with NC inhibitor or miR-21-5p inhibitor. n = 3. **D** qRT-PCR analysis of *p67phox*, *Gp91phox* and *Sod2* expression in NRCMs transfected with NC inhibitor or miR-21-5p inhibitor. n = 6. **E** Representative DHE staining images and statistical results. n = 6. Scale bar, 100 μm. Bars show mean ± SD. Data were compared by two-way ANOVA followed by Tukey's *post hoc* test. *, $p < 0.05$, **, $p < 0.01$, ***, $p < 0.001$. NC, negative control.

basic (Promega, Madison, WI) containing the binding site (or mutated) with miR-21-5p in the 3′UTR of BTG2. The BTG2 sequence was inserted at the *Xba*I restriction site in the pGL3-basic reporter vector. 293T cells were seeded in 24-well plates and transfected with 200 ng of indicated luciferase reporter constructs and 5 ng renilla plasmid as well as 2 μL miR-21-5p mimic (or NC mimic) using Lipofectamine™ 2000 (Invitrogen, MA, USA). Medium was changed 6–8 h after transfection. Cells were collected at 48 h after transfection and analyzed for luciferase activity. Dual-luciferase reporter assays were performed with the Dual-Luciferase Reporter Assay System (Promega, Madison, WI) according to the manufacturer's instructions. Firefly luciferase activity was normalized to the Renilla luciferase signal for further comparison.

2.9. Statistical methods

All data were analyzed by GraphPad Prism 8.0 statistical software. The statistical results were expressed as mean ± standard deviation (mean ± SD). An unpaired, two-tailed Student's t-test was used for comparisons between two groups. A two-way ANOVA test was performed to compare multiple groups followed by Tukey's *post hoc* test. $p < 0.05$ was considered to be statistically different.

3. Results

3.1. miR-21-5p was upregulated in DOX-treated primary neonatal rat cardiomyocytes and mouse heart tissues

To explore the functional roles of miR-21-5p in regulating DOX-induced cardiac injury, we first assessed the change of miR-21-5p expression level in NRCMs treated with DOX. A marked increase of miR-21-5p was observed in DOX-treated NRCMs (Fig. 1A). Furthermore, the expression level of miR-21-5p was also obviously increased in DOX-treated mouse hearts (Fig. 1B). These data suggested a possible functional role of miR-21-5p in the heart.

3.2. Overexpression of miR-21-5p inhibited DOX-induced apoptosis and oxidative stress in NRCMs

In order to determine the potential functional role of miR-21-5p in cardiomyocytes *in vitro*, we transfected NRCMs with miR-21-5p mimics or negative controls. After confirming that transfection of miR-21-5p mimic could efficiently increase miR-21-5p expression in NRCMs (Fig. 2A). We further detected DOX-induced cardiomyocyte apoptosis using TUNEL staining. Results showed that DOX treatment caused an obviously increased TUNEL-positive cardiomyocytes. However, the transfection of miR-21-5p mimic effectively reversed the pro-apoptotic effects of DOX treatment, indicating that miR-21-5p could attenuate DOX-induced cardiomyocyte apoptosis (Fig. 2B). We next examined DOX-induced cardiomyocyte apoptosis using Western blot for apoptosis-related proteins. Consistent with the TUNEL staining results, miR-21-5p mimic significantly decreased Bax/Bcl-2 ratio and cleaved-Caspase3/Caspase3 ratio in DOX-treated NRCMs (Fig. 2C). Meanwhile, miR-21-5p mimic remarkably decreased DOX-induced oxidative stress in NRCMs, as indicated by decreased mRNA levels of *p67phox* and *Gp91phox* as well as increased mRNA level of *Sod2* (Fig. 2D). DHE staining also verified the protective effect of miR-21-5p on DOX-induced oxidative stress (Fig. 2E). Altogether, these data provided direct evidence that increasing miR-21-5p suppressed cardiomyocyte apoptosis and oxidative stress in DOX-treated cardiomyocytes.

3.3. miR-21-5p inhibition increased cardiomyocyte apoptosis and oxidative stress

In order to further test the protective role of miR-21-5p in cardiomyocytes, the miR-21-5p inhibitor was used. The effect of miR-21-5p inhibitor in decreasing miR-21-5p was confirmed by qRT-PCR (Fig. 3A). Our study showed that the miR-21-5p inhibitor significantly increased TUNEL-positive cardiomyocytes (Fig. 3B). Meanwhile, miR-21-5p inhibitor transfection further increased Bax/Bcl-2 ratio and cleaved-Caspase3/Caspase3 ratio in DOX-treated NRCMs (Fig. 3C). Moreover, miR-21-5p inhibitor significantly increased DOX-induced oxidative stress in NRCMs while caused no significant change in oxidative stress under basal level (Fig. 3D and E). These data further confirmed that miR-21-5p could inhibit DOX-induced apoptosis and oxidative stress in NRCMs.

3.4. Therapeutic delivery of miR-21-5p reduced DOX-induced cardiac injury in mice

We next investigated the effect of miR-21-5p *in vivo*. Mice were injected with AAV9-miR-21-5p or AAV9-empty viruses, and then treated with DOX at a dose of 5 mg/kg per week through intraperitoneal administration for 4 weeks. One week after the fourth injection of DOX, mice were subjected to echocardiography (Fig. 4A). Here we observed that miR-21-5p was significantly increased in heart tissues of AAV9-miR-21-5p viruses-treated mice (Fig. 4B), and DOX treatment caused obviously lower heart weight-to-tibial length (HW/HL) ratio, which was effectively reversed by cardiac miR-21-5p overexpression (Fig. 4C). Meanwhile, we observed that

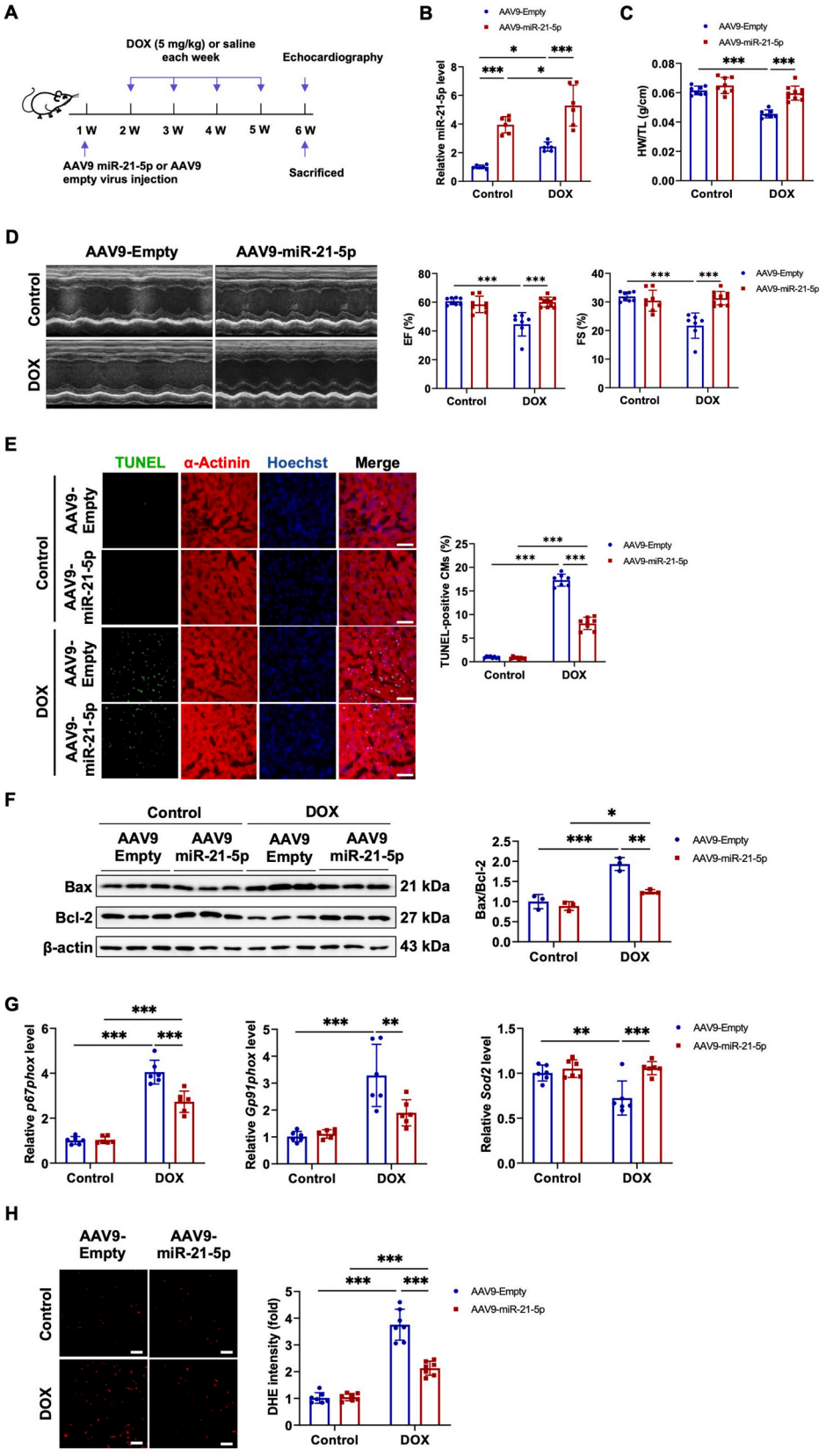

(caption on next page)

Fig. 4. miR-21-5p overexpression protected mice against DOX-induced myocardial injury. **A** Experimental design of virus injection and DOX treatment in mice, and time points of functional assessments. **B** qRT-PCR for miR-21-5p expression in heart tissues of mice treated with AAV9-Empty or AAV9-miR-21-5p viruses. n = 6. **C** Heart weight/tibia length (HW/TL) ratios of mice after four weeks of DOX treatment. n = 8:8:7:10. **D** Echocardiography for left-ventricular ejection fraction (EF, %) and fractional shortening (FS, %) in mice after four weeks of DOX treatment. n = 8:8:7:10. **E** TUNEL staining for myocardial apoptosis in α-actinin-labeled cardiomyocytes, n = 8:8:7:10. **F** Western blot analysis of Bax and Bcl-2 levels in heart tissues from DOX-treated mice. n = 3. **G** qRT-PCR analysis of *p67phox*, *Gp91phox* and *Sod2* expression in NRCMs transfected with NC inhibitor or miR-21-5p inhibitor. n = 6. **H** Representative DHE staining images and statistical results. n = 6. Scale bar, 50 μm. Bars show mean ± SD. Data were compared by two-way ANOVA followed by Tukey's *post hoc* test. *, $p < 0.05$, **, $p < 0.01$, ***, $p < 0.001$.

DOX treatment resulted in significant cardiac dysfunction, as evidenced by reduced EF and FS (Fig. 4D). On the contrary, mice with AAV9-mediated miR-21-5p overexpression in the heart had well-preserved cardiac function compared with the AAV9-Empty mice (Fig. 4D). Moreover, TUNEL staining analysis of heart tissues displayed significantly reduced TUNEL-positive cardiomyocytes in miR-21-5p overexpressing mice with DOX treatment (Fig. 4E). Meanwhile, Western blot analysis showed that miR-21-5p overexpression led to a reduced Bax to Bcl-2 ratio (Fig. 4F). Furthermore, miR-21-5p overexpression significantly decreased oxidative stress in heart tissues of DOX-treated mice (Fig. 4G and H). Taken together, these results demonstrated that therapeutic delivery of miR-21-5p had beneficial effects in attenuating cardiac dysfunction and apoptosis as well as oxidative stress in mice with DOX-induced cardiac injury.

3.5. miR-21-5p inhibited DOX-induced cardiomyocyte apoptosis by targeting BTG2

BTG2, a tumor suppressor gene, was previously reported as a target of miR-21-5p, which significantly decreased BTG2 levels in cultured cardiomyocytes [32]. BTG2 protein has been implicated in a variety of biological processes including cell division, DNA repair, and apoptosis in cancer cells [35,36]. To assess whether BTG2 is involved in the miR-21-5p-mediated cardioprotective effects, we first detected the level of BTG2 in mouse heart tissues. We observed that the protein expression level of BTG2 was obviously decreased in miR-21-5p overexpressing mouse hearts (Fig. 5A). Moreover, DOX treatment significantly reduced the BTG2 level. This result indicated that miR-21-5p could regulate the BTG2 expression in heart tissue under both normal and myocardial injury conditions. To further test whether miR-21-5p directly targets BTG2, we constructed luciferase reporter plasmids containing 3′ untranslated region (3′UTR) binding sequence or mutated sequence of BTG2. Co-transfection of miR-21-5p mimic with the plasmid containing BTG2 3′UTR binding sequence significantly reduced luciferase activity in 293T cells, while the decreased luciferase activity was recovered when the miR-21-5p binding site was mutated (Fig. 5B), indicating that miR-21-5p could directly target the 3′UTR of BTG2.

To further determine whether BTG2 mediated the anti-apoptotic effects of miR-21-5p, we transfected BTG2 overexpressing NRCMs with miR-21-5p mimic. As shown in Fig. 5C and D, overexpressing BTG2 abolished the beneficial effect of miR-21-5p mimic in reducing cardiomyocyte apoptosis. Additionally, lentivirus decreasing BTG2 attenuated the deleterious effect of the miR-21-5p inhibitor on cardiomyocyte apoptosis (Fig. 5E and F). Collectively, these data provided evidence that miR-21-5p inhibited DOX-induced cardiomyocyte apoptosis by downregulating BTG2.

4. Discussion

DOX is one of the widely used antitumor anthracyclines. Although DOX is effective in the treatment of various cancers, its clinical application is largely limited due to the life-threatening cardiotoxicity [3,37]. Our study adopted a low-dose chronic DOX treatment, which made the experimental conditions in line with the clinically chronic DOX-induced cardiomyopathy patients. miR-21-5p is one of the widely studied miRNAs in cancers, and the expression of miR-21-5p is obviously increased in various kinds of solid tumors [38]. miR-21-5p has been implicated in a variety of physiological processes, including cell proliferation, differentiation, and apoptosis, and is closely correlated with tumor growth, invasion, and metastasis [39–42]. Therefore, inhibition of miR-21-5p presents a promising strategy for cancer treatment. For example, it was shown that the combination treatment of DOX and miR-21-5p inhibitor markedly reduced cell proliferation, invasion, and migration in cultured tumor cells [43], which also indicated that combining DOX and miR-21-5p inhibitor represented a new strategy for cancer therapy. In addition, miR-21-5p could protect cardiomyocytes against ischemia-reperfusion (I/R) and hypoxia-reperfusion (H/R)-induced apoptosis [44,45]. Nucleolin was reported to protect cardiomyocytes from DOX-induced cardiac injury via upregulating miR-21-5p [46]. However, the functional role and the underlying mechanism of miR-21-5p in DOX-induced cardiomyopathy is still unclear.

Our study showed that miR-21-5p was significantly upregulated in DOX-induced cardiac injury. Increased miR-21-5p expression was able to inhibit DOX-induced apoptosis and oxidative stress in NRCMs, whereas decreased miR-21-5p expression promoted DOX-induced cardiomyocyte apoptosis and oxidative stress. Moreover, the cardiac expression of miR-21-5p was sufficient to protect the heart from DOX-induced cardiac injury. Mechanistically, miR-21-5p prevented cardiomyocyte apoptosis by downregulated BTG2. Our study indicated that miR-21-5p might serve as a therapeutic target for DOX-induced cardiomyopathy.

However, it is well known that miR-21-5p is increased in tumors, whilst its target BTG2 is decreased or mutated in tumors [47–49]. As a matter of fact, BTG2 is considered to be a tumor suppressor gene [35,36]. Therefore, decreasing the pro-apoptotic effect of DOX by further increasing miR-21-5p and further decreasing BTG2 expression might reduce the therapeutic effect of DOX. There might be a subtle edge whereby DOX concentration, miR-21-5p, and BTG2 expression could be tuned in order to minimize cardiomyocyte damage while supporting the anticancer effect of the drug. This may be investigated in future experiments using animal models of cancer.

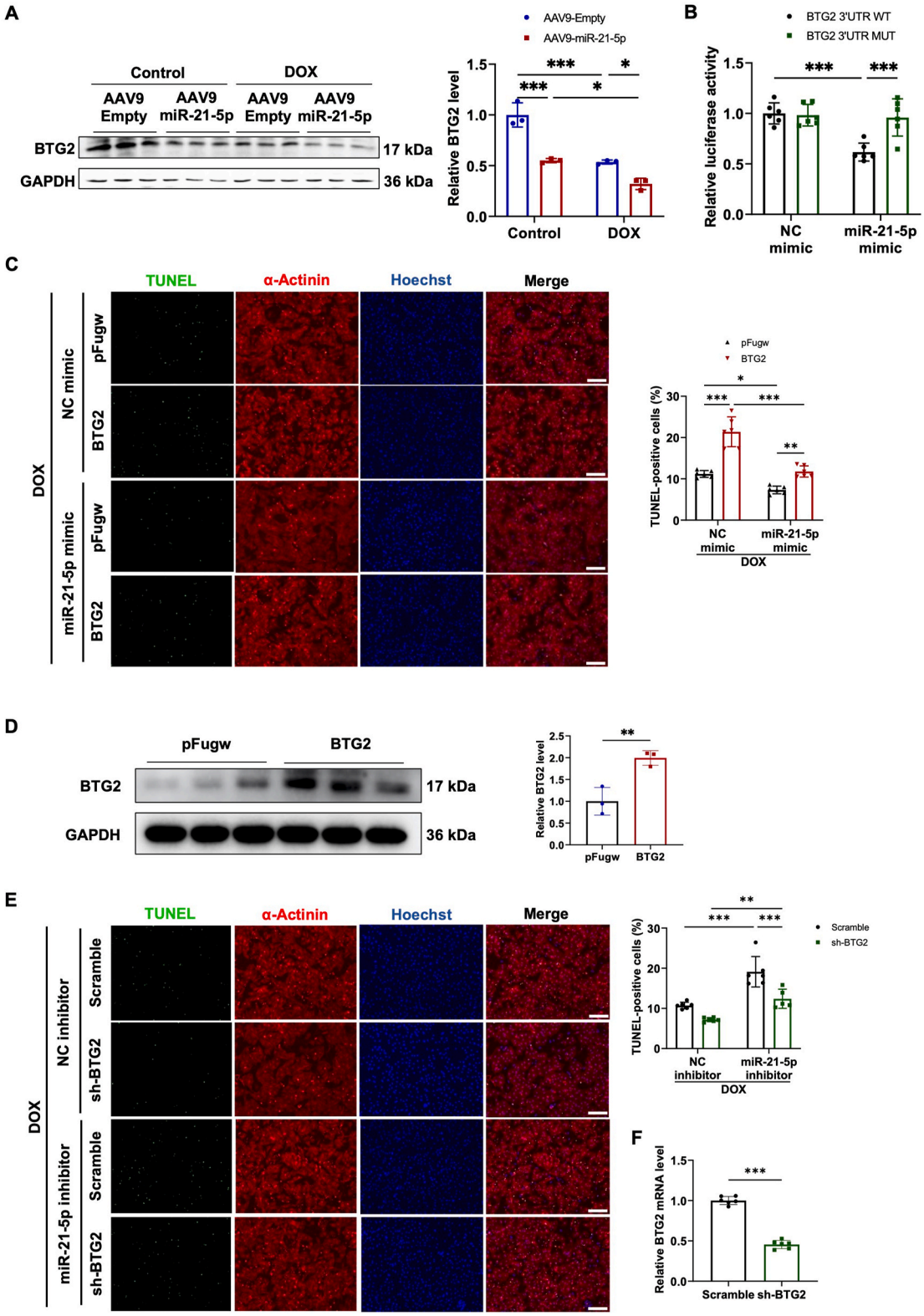

Fig. 5. miR-21-5p inhibited cardiomyocyte apoptosis by downregulating BTG2. **A** Western blot analysis of BTG2 levels in heart tissues from miR-21-5p overexpressing mice. n = 3. **B** Luciferase reporter assays performed in 293T cells transfected with miR-21-5p mimic (or negative control, NC mimic) and luciferase reporter plasmids containing the binding site in the 3′ UTR of BTG2 (BTG2 3′UTR WT) or the mutated binding site in the 3′ UTR of BTG2 (BTG2 3′UTR MUT). n = 6. **C** TUNEL staining for α-actinin-labeled NRCMs treated with miR-21-5p mimic and lentiviruses expressing

BTG2. n = 6. **D** Western blot analysis of BTG2 levels in NRCMs transfected with pFUGW or pFUGW-BTG2. n = 3. **E** TUNEL staining for α-actinin-labeled NRCMs treated with miR-21-5p inhibitor and lentiviruses downregulating BTG2. n = 6:6:6:5. **F** qRT-PCR analysis of BTG2 levels in NRCMs transfected with scramble or sh-BTG2 plasmid. n = 6. Scale bar, 100 μm. Bars show mean ± SD. Data were compared by two-way ANOVA followed by Tukey's *post hoc* test. *, $p < 0.05$, **, $p < 0.01$, ***, $p < 0.001$. NC, negative control.

5. Conclusion

Taken together, consistent with previous study [32], our study has shown that miR-21-5p could significantly inhibit DOX-induced apoptosis and oxidative stress in both primary cardiomyocytes and mouse heart tissues. Our mechanical study indicated that miR-21-5p prevented DOX-induced cardiomyocyte apoptosis by downregulating BTG2. However, the functional roles of miR-21-5p in DOX-induced cardiomyopathy deserve further exploration. For example, whether delivery of miR-21-5p shortly after DOX-induced cardiomyopathy still has a beneficial effect requires future investigation. In addition, it is worth to explore whether miR-21-5p levels are changed in DOX-treated patients. Despite the unknowns, the findings that miR-21-5p can ameliorate DOX-induced cardiac damage both *in vitro* and *in vivo* may shed light on new treatment of cardiovascular diseases.

Author contribution statement

Yan Qiu: Conceived and designed the experiments; Wrote the paper. Rongjing Ding: Conceived and designed the experiments. Qingwei Wang: Performed the experiments; Wrote the paper. Fei Jiang, Chenlin Zhao: Performed the experiments. Yicheng Lv, Yi Duan, Jiaxin Song, Meiyu Hu, Wenqian Fang: Analyzed and interpreted the data.

Funding statement

Rongjing Ding was supported by National Natural Science Foundation of China [81772446]. Wenqian Fang was supported by National Natural Science Foundation of China [82000371]. Dr Yan Qiu was supported by Sailing Program from Science and Technology Commission of Shanghai [21YF1413700].

Additional information

Supplementary content related to this article has been published online at [URL].

Availability of data and materials

All data can be obtained by contacting the corresponding authors.

Animal research ethical approval

All animal experiments were conducted under the established guidelines on the use and care of laboratory animals for biomedical research published by the National Institutes of Health (No. 85-23, revised 1996) and approved by the ethical committees of Shanghai University (approval number ECSHU 2021-074).

Consent to publish

All authors read and approved the final manuscript and submitted it for consideration for publication.

Declaration of competing interest

The authors declare that they have no known competing financial interests or personal relationships that could have appeared to influence the work reported in this paper.

Acknowledgments

Not applicable.

Appendix A. Supplementary data

Supplementary data to this article can be found online at https://doi.org/10.1016/j.heliyon.2023.e15451.

References

[1] K.T. Sawicki, et al., Preventing and treating anthracycline cardiotoxicity: new insights, Annu. Rev. Pharmacol. Toxicol. 61 (2021) 309–332.
[2] D. Cardinale, et al., Early detection of anthracycline cardiotoxicity and improvement with heart failure therapy, Circulation 131 (22) (2015) 1981–1988.
[3] P.K. Singal, N. Iliskovic, Doxorubicin-induced cardiomyopathy, N. Engl. J. Med. 339 (13) (1998) 900–905.
[4] M. Sheibani, et al., Doxorubicin-induced cardiotoxicity: an overview on pre-clinical therapeutic approaches, Cardiovasc. Toxicol. 22 (4) (2022) 292–310.
[5] N. Wenningmann, et al., Insights into doxorubicin-induced cardiotoxicity: molecular mechanisms, preventive strategies, and early monitoring, Mol. Pharmacol. 96 (2) (2019) 219–232.
[6] A. Bhagat, E.S. Kleinerman, Anthracycline-induced cardiotoxicity: causes, mechanisms, and prevention, Adv. Exp. Med. Biol. 1257 (2020) 181–192.
[7] T. Simunek, et al., Anthracycline-induced cardiotoxicity: overview of studies examining the roles of oxidative stress and free cellular iron, Pharmacol. Rep. 61 (1) (2009) 154–171.
[8] M.F. Xu, et al., Effects by doxorubicin on the myocardium are mediated by oxygen free radicals, Life Sci. 68 (8) (2001) 889–901.
[9] M.S. Horenstein, R.S. Vander Heide, T.J. L'Ecuyer, Molecular basis of anthracycline-induced cardiotoxicity and its prevention, Mol. Genet. Metabol. 71 (1–2) (2000) 436–444.
[10] Y. Octavia, et al., Doxorubicin-induced cardiomyopathy: from molecular mechanisms to therapeutic strategies, J. Mol. Cell. Cardiol. 52 (6) (2012) 1213–1225.
[11] Y.W. Zhang, et al., Cardiomyocyte death in doxorubicin-induced cardiotoxicity, Arch. Immunol. Ther. Exp. 57 (6) (2009) 435–445.
[12] H. Kitakata, et al., Therapeutic targets for DOX-induced cardiomyopathy: role of apoptosis vs. Ferroptosis, Int. J. Mol. Sci. 23 (3) (2022).
[13] M.L. Circu, T.Y. Aw, Reactive oxygen species, cellular redox systems, and apoptosis, Free Radic. Biol. Med. 48 (6) (2010) 749–762.
[14] J. Ni, et al., Trophoblast stem-cell-derived exosomes improve doxorubicin-induced dilated cardiomyopathy by modulating the let-7i/YAP pathway, Mol. Ther. Nucleic Acids 22 (2020) 948–956.
[15] J. Ni, et al., Human trophoblast-derived exosomes attenuate doxorubicin-induced cardiac injury by regulating miR-200b and downstream Zeb 1, J. Nanobiotechnol. 18 (1) (2020) 171.
[16] T.X. Lu, M.E. Rothenberg, MicroRNA, J. Allergy Clin. Immunol. 141 (4) (2018) 1202–1207.
[17] J.L. Johnson, Elucidating the contributory role of microRNA to cardiovascular diseases (a review), Vasc. Pharmacol. 114 (2019) 31–48.
[18] S.S. Zhou, et al., miRNAS in cardiovascular diseases: potential biomarkers, therapeutic targets and challenges, Acta Pharmacol. Sin. 39 (7) (2018) 1073–1084.
[19] F. Torma, et al., The roles of microRNA in redox metabolism and exercise-mediated adaptation, J. Sport Health Sci. 9 (5) (2020) 405–414.
[20] Y. Bei, et al., miR-486 attenuates cardiac ischemia/reperfusion injury and mediates the beneficial effect of exercise for myocardial protection, Mol. Ther. 30 (4) (2022) 1675–1691.
[21] N. Zeng, et al., Dickkopf 3: a novel target gene of miR-25-3p in promoting fibrosis-related gene expression in myocardial fibrosis, J. Cardiovasc. Transl. Res. 14 (6) (2021) 1051–1062.
[22] F. Chen, et al., MicroRNA-151 attenuates apoptosis of endothelial cells induced by oxidized low-density lipoprotein by targeting interleukin-17a (IL-17A), J. Cardiovasc. Transl. Res. 14 (3) (2021) 400–408.
[23] R.J. Henning, Cardiovascular exosomes and MicroRNAs in cardiovascular physiology and pathophysiology, J. Cardiovasc. Transl. Res. 14 (2) (2021) 195–212.
[24] I. Kawano, M. Adamcova, MicroRNAs in doxorubicin-induced cardiotoxicity: the DNA damage response, Front. Pharmacol. 13 (2022), 1055911.
[25] L. Zhao, et al., MicroRNA-140-5p aggravates doxorubicin-induced cardiotoxicity by promoting myocardial oxidative stress via targeting Nrf 2 and Sirt2, Redox Biol. 15 (2018) 284–296.
[26] J. Li, et al., miR-451 silencing inhibited doxorubicin exposure-induced cardiotoxicity in mice, BioMed Res. Int. 2019 (2019), 1528278.
[27] J.A. Pan, et al., miR-146a attenuates apoptosis and modulates autophagy by targeting TAF9b/P53 pathway in doxorubicin-induced cardiotoxicity, Cell Death Dis. 10 (9) (2019) 668.
[28] A.E. Jenike, M.K. Halushka, miR-21: a non-specific biomarker of all maladies, Biomark. Res. 9 (1) (2021).
[29] R. Kumarswamy, I. Volkmann, T. Thum, Regulation and function of miRNA-21 in health and disease, RNA Biol. 8 (5) (2011) 706–713.
[30] J. Zhang, et al., Overexpression of exosomal cardioprotective miRNAs mitigates hypoxia-induced H9c2 cells apoptosis, Int. J. Mol. Sci. 18 (4) (2017).
[31] L. Qiao, et al., microRNA-21-5p dysregulation in exosomes derived from heart failure patients impairs regenerative potential, J. Clin. Invest. 129 (6) (2019) 2237–2250.
[32] Z. Tong, et al., MiR-21 protected cardiomyocytes against doxorubicin-induced apoptosis by targeting BTG2, Int. J. Mol. Sci. 16 (7) (2015) 14511–14525.
[33] X. Liu, et al., miR-222 is necessary for exercise-induced cardiac growth and protects against pathological cardiac remodeling, Cell Metabol. 21 (4) (2015) 584–595.
[34] K.J. Livak, T.D. Schmittgen, Analysis of relative gene expression data using real-time quantitative PCR and the 2(-Delta Delta C(T)) Method, Methods 25 (4) (2001) 402–408.
[35] L. Yuniati, et al., Tumor suppressors BTG1 and BTG2: beyond growth control, J. Cell. Physiol. 234 (5) (2019) 5379–5389.
[36] B. Mao, Z. Zhang, G. Wang, BTG2: a rising star of tumor suppressors (review), Int. J. Oncol. 46 (2) (2015) 459–464.
[37] F.S. Carvalho, et al., Doxorubicin-induced cardiotoxicity: from bioenergetic failure and cell death to cardiomyopathy, Med. Res. Rev. 34 (1) (2014) 106–135.
[38] Y. Huang, et al., MicroRNA-21 gene and cancer, Med. Oncol. 30 (1) (2013) 376.
[39] S. Rossi, et al., microRNA fingerprinting of CLL patients with chromosome 17p deletion identify a miR-21 score that stratifies early survival, Blood 116 (6) (2010) 945–952.
[40] L.M. Moore, W. Zhang, Targeting miR-21 in glioma: a small RNA with big potential, Expert Opin. Ther. Targets 14 (11) (2010) 1247–1257.
[41] A.M. Krichevsky, G. Gabriely, miR-21: a small multi-faceted RNA, J. Cell Mol. Med. 13 (1) (2009) 39–53.
[42] S.D. Selcuklu, M.T. Donoghue, C. Spillane, miR-21 as a key regulator of oncogenic processes, Biochem. Soc. Trans. 37 (Pt 4) (2009) 918–925.
[43] S. Zhang, et al., Combination treatment with doxorubicin and microRNA-21 inhibitor synergistically augments anticancer activity through upregulation of tumor suppressing genes, Int. J. Oncol. 46 (4) (2015) 1589–1600.
[44] Q. Yang, K. Yang, A. Li, microRNA-21 protects against ischemia-reperfusion and hypoxia-reperfusion-induced cardiocyte apoptosis via the phosphatase and tensin homolog/Akt-dependent mechanism, Mol. Med. Rep. 9 (6) (2014) 2213–2220.
[45] Y. Song, et al., Localized injection of miRNA-21-enriched extracellular vesicles effectively restores cardiac function after myocardial infarction, Theranostics 9 (8) (2019) 2346–2360.
[46] H. Sun, et al., Nucleolin protects against doxorubicin-induced cardiotoxicity via upregulating microRNA-21, J. Cell. Physiol. 233 (12) (2018) 9516–9525.
[47] E. Leone, et al., Targeting miR-21 inhibits in vitro and in vivo multiple myeloma cell growth, Clin. Cancer Res. 19 (8) (2013) 2096–2106.
[48] V. Vandewalle, et al., miR-15a-5p and miR-21-5p contribute to chemoresistance in cytogenetically normal acute myeloid leukaemia by targeting PDCD4, ARL2 and BTG2, J. Cell Mol. Med. 25 (1) (2021) 575–585.
[49] R.D. Morin, et al., Frequent mutation of histone-modifying genes in non-Hodgkin lymphoma, Nature 476 (7360) (2011) 298–303.